A&A 644, A161 (2020)
https://doi.org/10.1051/0004-6361/202039020

Astronomy & Astrophysics

A Virgo Environmental Survey Tracing Ionised Gas Emission (VESTIGE)

VII. Bridging the cluster-ICM-galaxy evolution at small scales

A. Longobardi[1,⋆], A. Boselli[1], M. Fossati[2], J. A. Villa-Vélez[1], S. Bianchi[3], V. Casasola[4], E. Sarpa[5,6], F. Combes[7], G. Hensler[8], D. Burgarella[1], C. Schimd[1], A. Nanni[1], P. Côté[9], V. Buat[1], P. Amram[1], L. Ferrarese[9], J. Braine[10], G. Trinchieri[11], S. Boissier[1], M. Boquien[12], P. Andreani[13], S. Gwyn[8,9], and J. C. Cuillandre[14]

[1] Aix Marseille Univ., CNRS, CNES, LAM, Marseille, France
e-mail: alessia.longobardi@lam.fr
[2] Dipartimento di Fisica G. Occhialini, Universitá degli Studi di Milano Bicocca, Piazza della Scienza 3, 20126 Milano, Italy
[3] INAF – Osservatorio Astrofisico di Arcetri, Largo E. Fermi 5, 50125 Firenze, Italy
[4] INAF – Istituto di Radioastronomia, Via P. Gobetti 101, 40129 Bologna, Italy
[5] Dipartimento di Matematica e Fisica, Universitá degli studi Roma Tre, Via della Vasca Navale, 84, 00146 Roma, Italy
[6] INFN – Sezione di Roma Tre, Via della Vasca Navale 84, 00146 Roma, Italy
[7] Observatoire de Paris, Collège de France, PSL University, Sorbonne University, CNRS, LERMA, Paris, France
[8] Department for Astrophysics, University of Vienna, Türkenschanzstrasse 17, 1180 Vienna, Austria
[9] National Research Council of Canada, Herzberg Astronomy & Astrophysics Research Centre, 5071 W. Saanich Rd, Victoria, BC V9E 2E7, Canada
[10] Laboratoire d'Astrophysique de Bordeaux, Univ. Bordeaux, CNRS, B18N, Allée Geoffroy Saint-Hilaire, 33615 Pessac, France
[11] INAF – Osservatorio Astronomico di Brera, Via Brera 28, 20159 Milano, Italy
[12] Centro de Astronomía (CITEVA), Universidad de Antofagasta, Avenida Angamos 601, Antofagasta 1270300, Chile
[13] European Southern Observatory, Karl-Schwarzschild-Strasse 2, 85748 Garching, Germany
[14] 7 AIM, CEA, CNRS, Université Paris-Saclay, Université Paris Diderot, Sorbonne Paris Cité, Observatoire de Paris, PSL University, 91191 Gif-sur-Yvette Cedex, France

Received 24 July 2020 / Accepted 4 October 2020

ABSTRACT

Aims. We measure far-infrared (FIR) emission from tails of stripped dust following the ionised and atomic gas components in galaxies undergoing ram pressure stripping. We study the dust-to-gas relative distribution and mass ratio in the stripped interstellar medium and relate them to those of the intra-cluster medium (ICM), thus linking the cluster-ICM-galaxy evolution at small-scales. The galaxy sample consists of three Scd Virgo galaxies with stellar masses in the range of $10^9 \lesssim M_* \lesssim 10^{10}\,M_\odot$ and within 1 Mpc from the cluster centre, namely NGC 4330, NGC 4522, and NGC 4654.

Methods. Through the analysis of Virgo Environmental Survey Tracing Ionised Gas Emission (VESTIGE) Hα, *Herschel* SPIRE FIR, and VLA Imaging of Virgo in Atomic gas HI data, we trace the spatial distribution of the tails and infer the dust and gas masses from the measured FIR 250 μm and HI flux densities. Dust-to-gas mass ratios in the tails are analysed as a function of the galaxy mass, metallicity, and dust temperature.

Results. Along the stripped component, the dust distribution closely follows the HI and Hα emitting gas, which extend beyond the optical disc (defined by the B-band 25th magnitude isophote). In these regions, the dust-to-gas mass ratios are $2.0 \pm 0.6 \times 10^{-3}$, $0.7 \pm 0.1 \times 10^{-3}$, and $0.4 \pm 0.03 \times 10^{-3}$ for NGC 4330, NGC 4522, and NGC 4654, respectively. Thus, dust is widespread in the stripped material with a lower dust-to-gas mass ratio (up to a factor of 15) than the one measured in the main body of nearby galaxies. We also find a negative trend in the dust-to-gas mass ratio as a function of the metallicity that can be explained in terms of a dust component more centrally concentrated in more metal-rich systems. Together with the finding that the stripped dust is cold, $T_\mathrm{d} \lesssim 25$ K, our results can be interpreted as a consequence of an outside-in stripping of the galaxy interstellar medium.

Conclusions. Gas and dust in galaxies are perturbed in a similar fashion by the cluster environment, although their relative contribution differs from the one measured in the main body of the galaxies. When this value is considered, ram pressure stripping is consistent with being one of the key mechanisms in building up the Virgo intra-cluster component, injecting dust grains into the ICM, thus contributing to its metal enrichment.

Key words. galaxies: clusters: general – galaxies: clusters: individual: Virgo cluster – galaxies: clusters: intracluster medium – galaxies: evolution – galaxies: interactions – galaxies: ISM

1. Introduction

In a Λ cold dark matter (ΛCDM) universe, where the hierarchical evolution is the driving mechanism in determining the current epoch characteristics of galaxies, it is expected that an abundance of low surface brightness, intra-cluster tidal debris from disrupted systems, and an ubiquity of diffuse structures permeate the intra-cluster medium (ICM) of galaxy clusters (e.g. Napolitano et al. 2003; Murante et al. 2004; Sommer-Larsen et al. 2005). In fact, as a consequence of environmental processing, when a galaxy enters a high-density

⋆ AL acknowledges support from the French Centre National d'Etudes Spatiales (CNES).

region, it can be subjected to gravitational interactions with other galaxies or with the potential well of the over-dense region or, alternatively, it can feel the pressure exerted by the hot and dense ICM (Boselli & Gavazzi 2006). Baryons are stripped from the main body of the galaxies, resulting in the production of tails of stripped material. This history is often hidden, however, being at surface brightness levels much fainter than the sky. It is only thanks to advances in sensitivity as well as in angular and spatial resolution of modern multi-frequency instrumentation that astronomers have been able to collect growing evidence of objects undergoing stripping in the different phases of the interstellar medium (ISM). Long tails of atomic gas have been detected and interpreted to be the result of the stripping of the, more extended, galaxy HI disc (e.g. Chung et al. 2009). In some cases, this gas also appears as ionised (hotter) and is detected through its Hα emission (e.g. Boselli et al. 2016; Poggianti et al. 2017; Fossati et al. 2018; Bellhouse et al. 2019), or it may get heated to the cluster X-ray temperature (Sun et al. 2006). Finally, cold molecular gas, which is usually detected through its CO emission, has been found to follow the stripped HI component (e.g. Vollmer et al. 2008; Verdugo et al. 2015; Jáchym et al. 2017; Moretti et al. 2018, 2020; Cramer et al. 2020; Zabel et al. 2019).

Since the dust is also perturbed by environmental processing (e.g. Cortese et al. 2010a,b; Kenney et al. 2015; Abramson et al. 2016) and in galaxies it is associated with the gaseous component of the ISM, it is generally expected that part of the dust is removed together with the gas during stripping. Several studies in the literature have identified dust in absorption in stripped tails through the analysis of the Balmer decrement. However, since it is associated with extra-planar HII star-forming regions, this is likely formed in situ (e.g Fossati et al. 2016; Poggianti et al. 2017, 2019; Gullieuszik et al. 2017; Bianconi et al. 2020). Thus, to which extent the dust follows the same fate as the stripped hydrogen is still an open question. We do not know whether the dust-to-gas ratios in the stripped tails of systems undergoing environmental processing differ from those measured in the main body of the galaxies. Thus, we do not know whether the properties between the different phases of the ISM change during the different stages of evolution. Additionally, if the stripped tails lie outside the galaxies' optical discs, they are likely going to be removed from the cluster spirals and to build up the cluster intra-cluster component (ICC).

This work aims at bridging the cluster-ICM-galaxy evolution at small scales by analysing the relative fraction in mass of the different baryonic components in the stripped ISM of galaxies subject to environmental processes. Our study targets galaxies in the Virgo cluster, that is the nearest large concentration of mass; furthermore, it is a dynamically young cluster (e.g. Binggeli et al. 1987; Böhringer et al. 1994) for which an exceptional collection of multi-frequency data at good and optimal resolution and sensitivity is available. In this context, the Virgo Environmental Survey Tracing Ionised Gas Emission (VESTIGE; Boselli et al. 2018) is a new, blind Hα survey providing us with the largest and most in-depth information on the ionised gas emission in Virgo, revealing unknown tails of stripped gas in several cluster members. Additionally, the Virgo cluster has recently been shown to contain a diffuse IC dust (ICD) component that is widespread in the cluster ICM with a dust-to-gas mass ratio of $M_{\rm d}/M_{\rm g} = 3.0 \pm 0.3 \times 10^{-4}$ and it is likely transported into the IC space by stripping (Longobardi et al. 2020).

Throughout the paper, we consider the cluster centred on M 87, with a virial radius of $r_{\rm vir} = 1.55$ Mpc (McLaughlin 1999). By assuming a flat ΛCDM universe with $\Omega_{\rm M} = 0.3$, $\Omega_\Lambda = 0.7$, $H_0 = 70\,{\rm km\,s^{-1}\,Mpc^{-1}}$, and a distance for Virgo of 16.5 Mpc (Gavazzi et al. 1999; Mei et al. 2007; Blakeslee et al. 2009), the adopted physical scale is 80 pc arcsec^{-1}. The optical disc extention refers to the B-band 25th magnitude isophote.

2. Photometric data

The data comes from a compilation of multi-wavelength campaigns surveying the Virgo cluster in the ultraviolet (UV), optical, radio, and far-infrared (FIR). In what follows, we give a brief description of these surveys and refer the reader to the references therein for additional details.

2.1. The VESTIGE survey

VESTIGE is a blind survey of the Virgo cluster carried out with MegaCam on the Canada-France-Hawaii Telescope (CFHT) with the Hα narrow band filter[1] and the broad-band r' filter (Boselli et al. 2018). It is designed to cover a total area of 104 deg^2 and reach the two main subclusters (Virgo A centred on M 87 and Virgo B centred on M 49) out to their virial radii. Currently the survey covers 40% of the designed area at full depth with the current observations taken in excellent weather conditions (median seeing ∼0.62″ and 0.65″ in the narrow-band and r'-band filter, respectively). VESTIGE data have been reduced using the Elixir-LSB package (Ferrarese et al. 2012), which is optimised for the removal of the instrumental background and scattered light from the science frames. This provides a high signal-to-noise ratio of the extended low surface brightness features, making VESTIGE a deep photometric survey, which for extended sources reaches a depth of $\Sigma({\rm H}\alpha) \sim 2\times10^{-18}$ erg s^{-1} cm^{-2} arcsec^{-2} at 3″ resolution. The photometric zero points were tied to Pan-STARRS photometry for both filters with a final photometric uncertainty of ∼2−3% (see Boselli et al. 2018). All final images have the same astrometric reference frame, which is tied to the positions of stars in the Sloan Digital Sky Survey (SDSS), with a spatial scale of 0.186″ px^{-1} (Gwyn 2008). Finally, Hα images with the only nebular line contribution are obtained via the subtraction of stellar continuum. The latter is obtained scaling the r'-band image by a $(g'-r')$ colour factor that accounts for the difference in the central wavelength of the narrow and broad band filters (see Boselli et al. 2018, 2019, 2020; Fossati et al. 2018). The optical g'-band information is taken from the Next Generation Virgo Cluster Survey (Ferrarese et al. 2012), which we describe below.

2.2. The NGVS survey

The broad band optical information is taken from the Next Generation Virgo Cluster Survey (NGVS; Ferrarese et al. 2012), a deep CFHT programme in the u^*, g', i', and z' bands, which covers a total area of 104 deg^2 in Virgo. The data were reduced with the Elixir-LSB pipeline and the photometric zero points were tied to SDSS photometry, as was done for the VESTIGE data. The typical full-width-half-maximum (FWHM) is ∼0.55″ in the i' band and ∼0.8″ in the other bands. In the g' band, the NGVS reaches a depth for extend sources of $g' = 27.7$ mag arcsec^2.

2.3. The HeViCS survey

Far-infrared data come from the *Herschel* Virgo Cluster Survey (HeViCS; Davies et al. 2010), a programme that covers ∼60 deg^2

[1] Given the characteristics of the CFHT Hα filter (central wavelength $\lambda_{\rm c} = 6591$ Å and a bandwidth of 106 Å), the VESTIGE data include [NII] line contribution.

of the Virgo cluster using the PACS (Poglitsch et al. 2010) instrument at 100 and 160 μm as well as the SPIRE (Griffin et al. 2010) instrument at 250, 350, and 500 μm. Data were integrated into the *Herschel* Reference Survey (HRS; Boselli et al. 2010), and their reduction was carried out as described in Ciesla et al. (2012) and Cortese et al. (2014). The sensitivity and FWHMs of the PACS observations are ~6.8 and ~3.1 MJy sr^{-1} and 7″ and 12″ at 100 and 160 μm, respectively, while the sensitivity and FWHMs of the SPIRE observations are ~1.0, 0.8, and 1.0 MJy sr^{-1} and ~18″, ~25″, and ~36″ at 250, 350, and 500 μm, respectively. Among these, the FIR 250 μm observations are the only ones that allow for a statistically significant measurement of the fluxes in the tail regions due to a compromise between spatial resolution and depth (see Sect. 4.1). As a result of this, the main photometric analysis in Sect. 4 is only based on SPIRE 250 μm data, for which the adopted beam size value is the pipeline beam solid angle equal to 469.35 arcsec^2.

2.4. The VIVA survey

The VLA Imaging of Virgo in Atomic gas (VIVA) survey is an imaging survey in HI of 53 Virgo late-type galaxies, covering angular distances of ~1−12 deg (~0.3−3.5 Mpc) from the cluster's centre (Chung et al. 2009). The total HI image, the intensity weighted velocity field, and the velocity dispersion image were produced using the Astronomical Imaging Processing System (AIPS) by taking moments along the frequency axis (the 0th, 1st, and 2nd moment). This resulted in an HI imaging survey with a typical spatial resolution of 15″ and a column density sensitivity of about 3−5 × 10^{19} cm^{-2} (3σ) per 10 km s^{-1} channel. For our sample of objects (see the next section), the beam FWHMs are 26.36″ × 23.98″, 18.88″ × 15.20″, and 16.14″ × 15.52″ for NGC 4330, NGC 4522, and NGC 4654, respectively.

2.5. The GUViCS survey

The GALEX Ultraviolet Virgo Cluster Survey (GUViCS; Boselli et al. 2011) presents GALEX far-UV (FUV) and near-UV (NUV) observations of the Virgo cluster. It combines data from the All-sky Imaging Survey (~5″ spatial resolution and single-exposure times of typically 100 s) and the Medium Imaging Survey (MIS; same spatial resolution, but with deeper exposure times of at least 1500 s), processed with the GALEX pipeline (Bianchi 2014).

3. The galaxy sample

To study the interplay between gas and dust during a late stage of galaxy evolution and its connection with the building up of the Virgo ICC, our study samples galaxies with tails of ionised Hα, neutral HI, and FIR emission, extending beyond the galaxy's optical disc, namely NGC 4330, NGC 4522, and NGC 4654. They are all galaxies of Scd morphological type, located within 4 deg (~1 Mpc) from the cluster centre, and with intermediate stellar masses in the range of $10^9 \lesssim M_* \lesssim 10^{10}\ M_\odot$. Table 1 lists some of the physical properties of the galaxy sample.

NGC 4330 shows truncated discs in UV and Hα (e.g. Vollmer et al. 2020; Fossati et al. 2018), FIR (Cortese et al. 2010a), HI (Chung et al. 2009; Abramson et al. 2011), and CO (Lee et al. 2017) on the north-east side of the stellar disc, and it shows a low surface-brightness as well as extended tails of ionised and neutral atomic gas on the southern side. It is a clear example of a galaxy undergoing ram pressure stripping that is effectively quenching the star formation activity with an out-in radial gradient (Fossati et al. 2018). NGC 4522 is farther away in projected distance from the centre of the cluster (0.9 Mpc); however, it still experiences ram pressure stripping as indicated by the HI and CO asymmetric morphology (Vollmer et al. 2006, 2008; Chung et al. 2009). Finally, NGC 4654, at the same distance of NGC 4522, shows HI and CO gas distributions compressed in the north-west, but very extended HI gas on the opposite side (CO observation do not extend at such distances; Chung & Kim 2014). The stellar and Hα morphologies are also asymmetric, showing an enhancement of ionised emission in the north-west, which is representative of recent star formation in this region (Chung et al. 2007), as well as tails of stripped stars in the south-east. As a result of these characteristics, NGC 4654 may be the only case in our sample of galaxies undergoing both ram pressure and tidal stripping, as has also been suggested by the theoretical models of Vollmer (2003).

We stress that this sample is not complete. NGC 4330, NGC 4522, and NGC 4654 represent 40% of the Virgo galaxies with Hα, HI, and FIR tails, and only ~5% of the galaxies that are expected to be subject to ram pressure stripping in Virgo (Boselli & Gavazzi 2014). The following three main factors led to this incompleteness. First, the VESTIGE survey has reached full sensitivity only in the central 5° of the cluster, thus it does not allow for a complete comparison with the VIVA sample; the latter extends out to the edge of the cluster. Second, our sample is biased towards bright and massive galaxies: Only ten VIVA targets are classified as Sd/Sm/Im galaxies and 50% of these lie outside the VESTIGE complete region. Third, for the remaining fraction of low mass galaxies within the sampled area, the current sensitivity and resolution of the FIR observations are likely prohibitive to detect stripped dust tails. However, these objects are expected to be the most affected by environmental processes. Even though it is limited in statistics, our work is to be considered a pilot study for future campaigns.

4. Stripped tails

Truncated discs of gas and dust due to environmental effects have already been investigated in the past (e.g. Chung et al. 2009; Cortese et al. 2016, 2010a; Lee et al. 2017). Here, we focus on the novelty of the present study, that is, the identification of more extended Hα tails, the detection of diffuse FIR emission of dust tails, and their connection with the HI gas component.

In Fig. 1 we compare the g'-band, Hα, FIR 250 μm, and HI maps for our sample of galaxies, where we smoothed the original Hα and FIR images with a Gaussian kernel of 2.5″ and 12″, respectively, to better show the faint structures. In Hα, FIR, and HI, these galaxies are morphologically asymmetric. Furthermore, by comparing the gas and dust distributions with the optical disc extension (white ellipses in Fig. 1), in addition to the well-known truncated discs in Hα, FIR, and HI, a component is visible that extends outside the optical radius. These features are very faint in Hα and FIR, reaching the respective survey sensitivity limits in both bands.

NGC 4330. The previously detected Hα and HI tails bending to the south in the downstream region of NGC 4330, together with the Hα low surface brightness filaments that extend further from the tail to the south (e.g. Chung et al. 2009; Fossati et al. 2018), are followed by a tail of dust emitting in the FIR that extends out to 6 kpc from the galaxy disc, which has never been detected before. Superimposed to the Hα emission in the tail are

Table 1. Physical properties of the galaxy sample.

ID	RA	Dec	D_{25} [a]	i [a]	v [a]	d_{M87}	log M_* [a]	log M_{dust} [b]	log M_{HI} [c]	$L_{H\alpha}$	$S_{250\,\mu m}$	S_{HI}	def$_{HI}$ [c]
	J2000	J2000	(arcmin)	(deg)	(km s^{-1})	(Mpc)	($M_\odot$)	($M_\odot$)	($M_\odot$)	(10^{40} erg s^{-1})	(Jy)	(Jy km s^{-1})	
(1)	(2)	(3)	(4)	(5)	(6)	(7)	(8)	(9)	(10)	(11)	(12)	(13)	(14)
NGC 4330	12:23:17.25	+11:22:04.7	5.86	90	1567	0.6	9.3	6.9	8.7	1.1 ± 0.02	3.0 ± 0.5	39.7±7.4	0.80
NGC 4522	12:33:39.66	+09:10:29.5	4.04	79	2332	0.9	9.3	6.9	8.8	1.4 ± 0.03	2.9 ± 0.3	59.4 ± 11.9	0.86
NGC 4654	12:43:56.58	+13:07:36.0	4.99	56	1035	0.9	10.2	7.8	9.5	19.2 ± 0.01	24.8 ± 0.9	73.3 ± 14.7	0.12

Notes. Column 1: Galaxy name. Columns 2 and 3: J2000 coordinates. Column 4: Optical size defined by the B-band 25th magnitude isophote. Column 5: Inclination angle. Column 6: Velocity. Column 7: Projected distance from M 87. Columns 8−10: log values of stellar, dust, and HI gas masses. Column 11: Total luminosity in Hα within D_{25}. Columns 12 and 13: Total FIR 250 μm and HI flux densities within D_{25}. Column 14: HI-def parameter measured as the logarithmic difference between the expected and observed HI masses. [a]Cortese et al. (2012). [b]Ciesla et al. (2012). [c] Chung et al. (2009). The M_{HI} values were scaled to take the different distances assumed for the Virgo cluster into account.

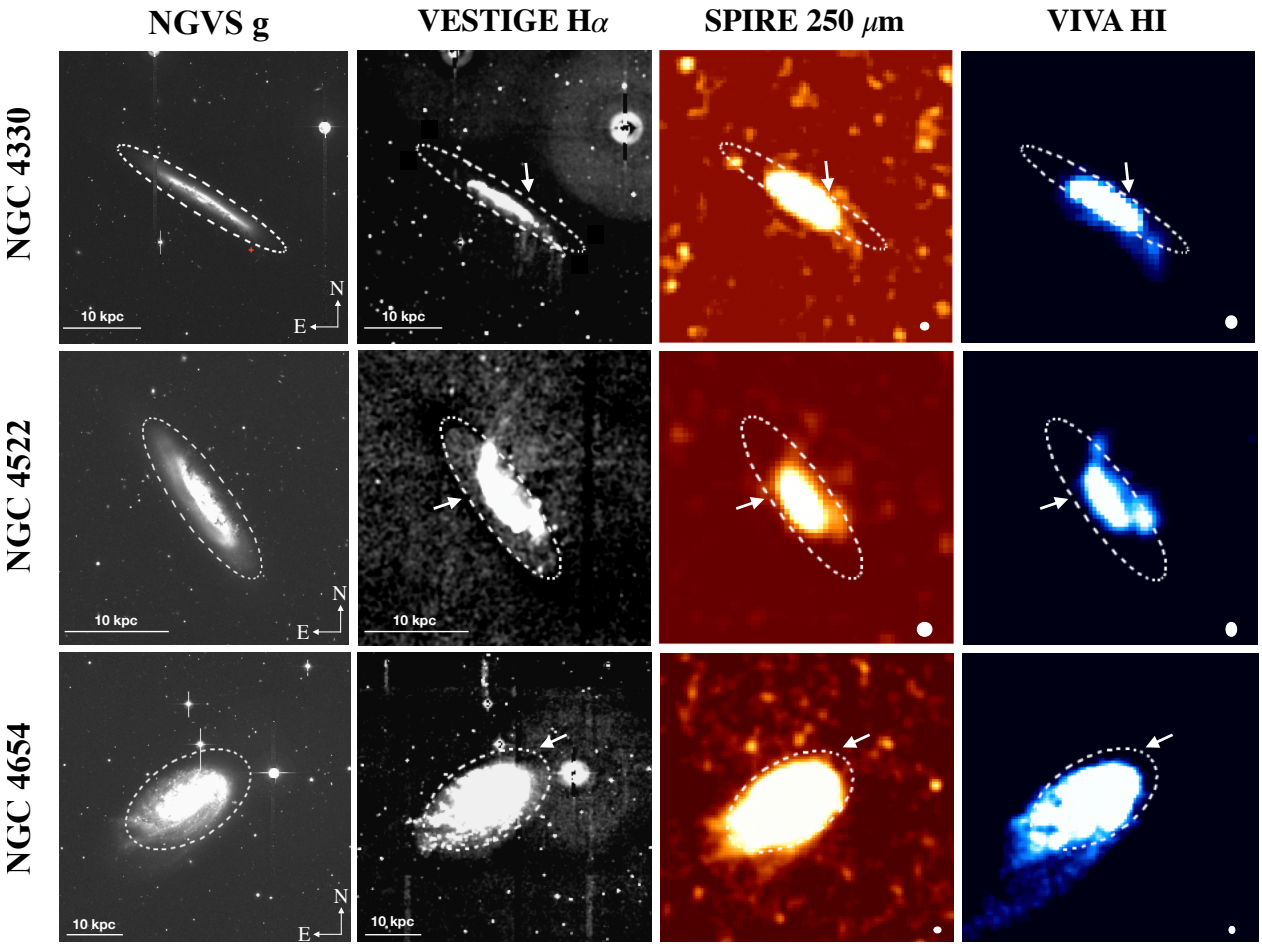

Fig. 1. g'-band, Hα, FIR 250 μm, and HI maps for the galaxies in our sample. The Hα and FIR 250 μm images were smoothed by a Gaussian kernel of 2.5″ and 12″, respectively. Tails of stripped material extending beyond the optical disc (dotted ellipse) are visible in the Hα, FIR 250 μm, and HI bands. White arrows indicate the wind direction (Vollmer 2003; Lee et al. 2017). The red cross in the g'-band image of NGC 4330 identifies the background contaminant (see text). North is up; east is to the left.

regions of recent star formation, which are better seen in Fig. 2 where the VESTIGE Hα image is compared to GUViCS FUV emission from young stars (magenta contours). These features have been previously identified by several authors in the past (Abramson et al. 2011; Boissier et al. 2012; Fossati et al. 2018), and they can also be explained by a stripped dust component that cools the gas ablated from the disc and leads to episodes of star formation. The correlation between the ionised gas, dust (red contours), and the HI emission (blue contours) shown in Fig. 2 may support this hypothesis. Furthermore, the atomic gas and dust display similar extensions to that of the ionised gas, also covering the region where the low surface brightness Hα filaments appear. On the contrary, the FUV emission is limited to the downstream tail and does not cover the regions extending further south, suggesting that we may expect ionised Hα emission to have another origin than photoionisation. In this scenario, the tail hosts massive star formation, which ionises the cool gas producing Hα emission, while the southern filaments result from the ionisation of stripped atomic gas from thermal conduction or shock-heating due to the interaction with the hot ICM, as has

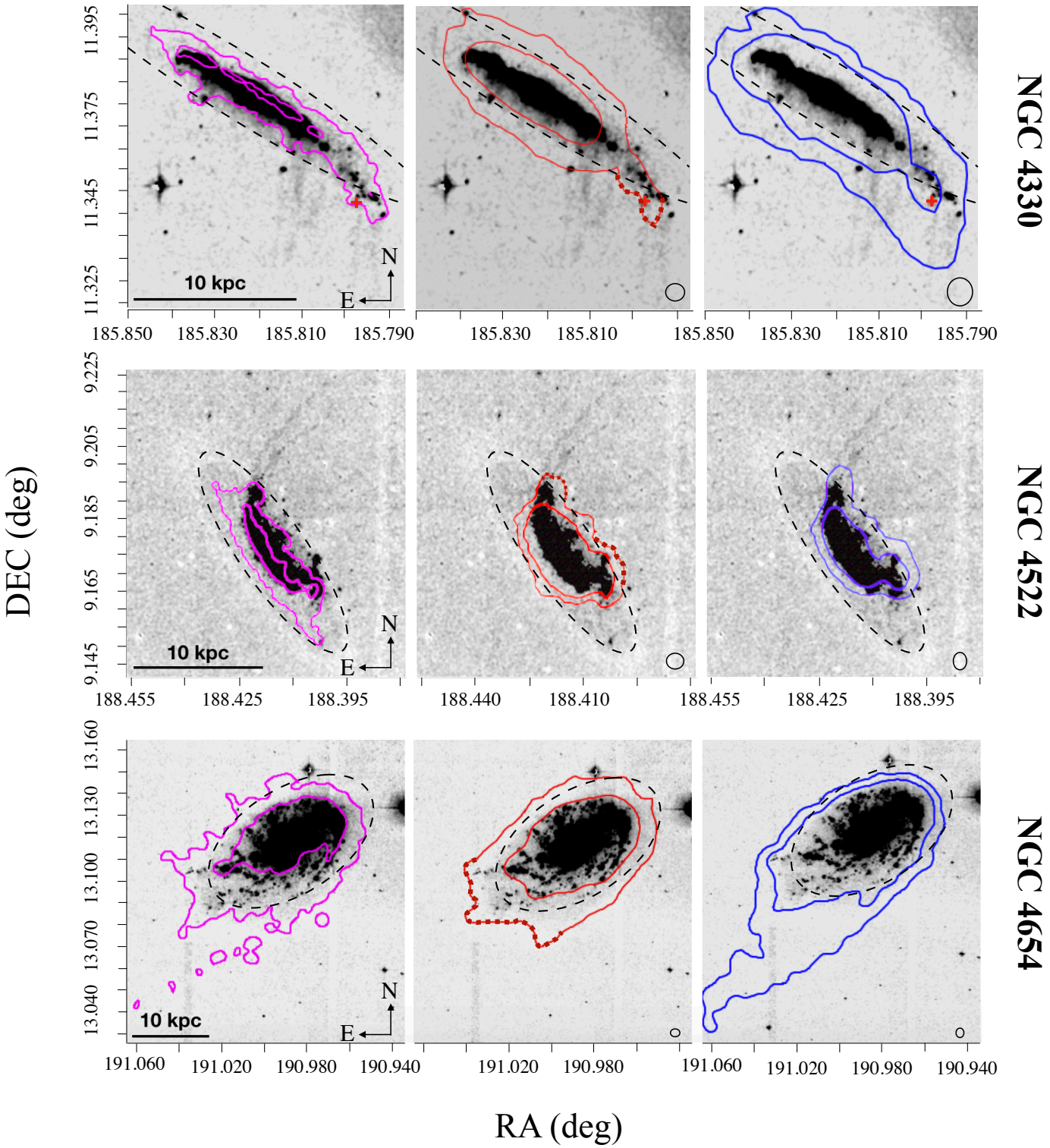

Fig. 2. Smoothed Hα VESTIGE images of NGC 4330 (*top*), NGC 4522 (*centre*), and NGC 4654 (*bottom*) compared with the GALEX FUV emission (magenta contours), SPIRE 250 μm emission (red contours), and VIVA HI emission (blue contours). The faintest emissions from the SPIRE 250 μm data are at surface brightness levels of 0.6 MJy sr^{-1}, while the HI contour levels reach column densities values of $\Sigma_{HI} = 2{\times}10^{19}$ cm^{-2}. Dotted black ellipses trace the extensions of the galaxies' optical discs. The regions of the tails outside the optical disc are considered for our photometric analysis (red dotted contours). Linear scales and synthesised beam sizes are shown in the bottom-left and bottom-right corners, respectively.

recently been confirmed in the theoretical work of Vollmer et al. (2020) on NGC 4330 and as has been found in other ram pressure tails (Fossati et al. 2016) or simulations (Tonnesen & Bryan 2012). Finally, the morphology of the filaments, their length, width, and clumpiness may result from the presence of magnetic pressure (Fossati et al. 2018), as can also be seen in